

Voltage and frequency stabilization by fuzzy integrated droop control of a multi renewable source micro grid

Savitri Swathi¹, Bhaskaruni Suresh Kumar², Jalla Uppendar¹

¹Department of Electrical Engineering, University College of Engineering, Osmania University, Hyderabad, India

²Department of Electrical and Electronics, Osmania University, Hyderabad, India

Article Info

Article history:

Received Oct 16, 2022

Revised Jan 19, 2023

Accepted Feb 4, 2023

Keywords:

Droop control

Fuzzy interference structure

MATLAB

Proportional integral and derivative

Simulink

Synchronous reference frame

ABSTRACT

A multi renewable source micro-grid system has many power quality issues when it is operated in grid islanding condition. During grid connected mode the voltage and frequency of the system will remain stable for small disturbances like load changes or environmental changes. During these sudden variations in the system, the grid supports the load maintaining the system stable. In this paper a droop control is introduced for the renewable source module 3-ph inverter during standalone mode supporting the load. For detection of grid islanding, an active islanding detection control is adopted which makes the 3-ph inverter to shift from synchronous reference frame (SRF) control to droop control. The performance of the droop control is improvised with fuzzy interference structure (FIS) module replacing the conventional proportional integral and derivative (PID) control. A comparative analysis is done in this paper with different controllers in droop control scheme using matrix laboratory (MATLAB) Simulink software. Stability analysis is carried out on the system determining the voltage and frequency fluctuations during grid disturbances. There is an improvement in load compensation, voltage ripple, voltage magnitude, frequency ripple and settling time with the introduced fuzzy droop controller.

This is an open access article under the [CC BY-SA](https://creativecommons.org/licenses/by-sa/4.0/) license.



Corresponding Author:

Savitri Swathi

Department of Electrical Engineering, University College of Engineering, Osmania University
Hyderabad, India

Email: eee.swathi48@gmail.com

1. INTRODUCTION

For clean and green electrical power generation most of the grids as of today and in future are adopting renewable sources. The grid is bifurcated into multiple micro-grids [1] where each micro-grid is introduced with local renewable sources. Different renewable source like photovoltaic (PV) system, wind farms or fuel cells can be used for compensation of local load demand. In most of the previous research the renewable sources are always grid connected which share power to the load along with main grid. The grid connected condition have very less power quality issues as the main grid always supports the system for any sudden or intermittent disturbances. The major issues transpire when the system is alienated [2] from main grid making it to work in standalone condition during main grid failure. During grid connected mode the renewable source module 3-ph inverter is operated using synchronous reference frame (SRF) control which takes feedback from the grid side 3-ph voltages. The SRF control uses phase locked loop (PLL) unit for the operation of the 3-ph inverter to synchronize with the grid voltages for sharing of renewable power [3]. In the grid connected mode the system has better stability even during sudden load changes or renewable power disturbances as the main source supports the system. The voltage, frequency, and powers of all the modules are maintained with less

disturbance or oscillations. A simple renewable source micro-grid interconnected to main grid schematic can be observed in Figure 1.

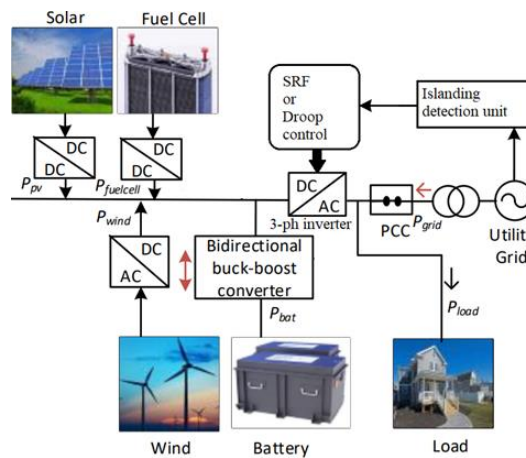


Figure 1. Renewable micro-grid test system

In the given test system as in Figure 1 the renewable source micro-grid is included with boost-converter PV module, boost converter fuel-cell module, AC-DC converter wind farm module and bidirectional converter battery pack for power backup. All these renewable source modules are interlinked to a DC bus where 3-ph inverter is connected injecting renewable power to grid. The 3-ph inverter is either operated with SRF or droop control as per the grid available condition. The 3-ph inverter controller selection is done by islanding detection unit [4]–[6] which identifies the utility grid connection to the renewable micro-grid. The powers of the four renewable modules are utilized as per load demand and grid connection conditions.

The contents of this paper include introduction in section 1 followed by configuration of four modules renewable micro-grid in section 2. In section 3 the control structure design for the control of 3-ph inverter is discussed which includes SRF control and droop control in grid connected mode and islanding mode respectively. The section 3 is also included with islanding detection algorithm which determines the 3-ph inverter control operation. Section 4 is the simulation results analysis and graphical representation of different measurements. The analysis of the proposed system is done with different operating conditions and parametric stability comparisons are shown. The comparison includes different controllers in droop control structure which are PI, PID, and FIS. The final section 5 is conclusion to this paper where the optimal controller for the 3-ph inverter is determined with tabular comparison, followed by references given in this paper.

In previous researches [2]–[4] droop controllers are introduced to fixed DC sources or stable sources which compensate the required load. The stability of the controller is tested when the stable DC sources are replaced with unpredictable renewable sources. The response time of the droop controller needs to be tested [5] with different operating conditions and source failures. The peak overshoots and disturbances caused by the conventional PI controller needs to be mitigated with new robust advanced control modules.

2. RENEWABLE MICRO GRID CONFIGURATION

As mentioned previously in section 1 the renewable micro-grid is included with four source modules which operate as per the grid connection condition. From the four sources, PV module and wind farm module are the major renewable sources [7] which generate power utilizing solar irradiation and natural winds. The powers from these two sources PV and wind farm are completely extracted in any operating condition of the grid. As these sources generate power from natural resources it is recommendable to extract the total power that they are generating which can be either fed to load, grid or can be stored in battery module. The third renewable source is fuel cell which generates power using specific hydrogen and oxygen provision as per the requirement. This fuel cell is an optional source as the power generation can be controlled and can be activated during demand. The fourth source is otherwise called as energy storage module which comprise of battery pack [8]. This battery pack can store power from excess generation by the photovoltaic and wind farm modules. The complete structure of the micro-grid with four sources with their controllable power electronic devices is shown in Figure 2.

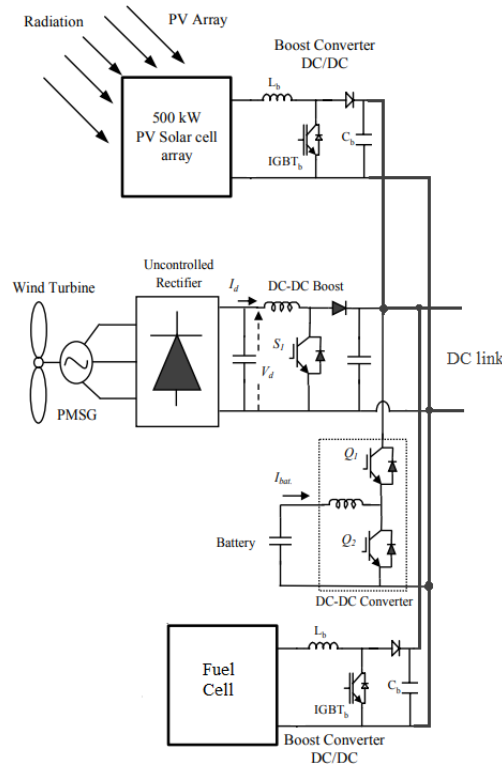


Figure 2. Proposed four source micro-grid

As per the Figure 2 micro-grid configuration the PV source and fuel cell sources are connected to individual boost converters for boosting the voltage as per the requirement. The wind farm module has a permanent magnet synchronous generator (PMSG) which is an independent power generation machine. Even the wind farm uses boost converter but with a diode bridge rectifier between PMSG and the converter for AC-DC conversion [9], [10]. The battery module comprises of a bidirectional DC-DC converter which has the capability to store and extract power from battery during excess and deficit conditions respectively. All these converters are connected to common DC link for power sharing to the grid through a 3-ph inverter.

The boost converter of the PV unit is controlled using traditional perturb and observe (P&O) maximum power point tracking (MPPT) control algorithm [11]. This technique is most adopted control in many systems because of its simple logic with respect to PV source voltage and current. The duty ratio of the boost converter is either increased or decreased as per the change in PV voltage and current parameters which are impacted by solar irradiation:

$$D = D_1 + \Delta D; \begin{cases} \text{If } P(k) > P(k - 1) \text{ and } V(k) > V(k - 1) \\ \text{If } P(k) < P(k - 1) \text{ and } V(k) < V(k - 1) \end{cases} \quad (1)$$

$$D = D_1 - \Delta D; \begin{cases} \text{If } P(k) > P(k - 1) \text{ and } V(k) < V(k - 1) \\ \text{If } P(k) < P(k - 1) \text{ and } V(k) > V(k - 1) \end{cases} \quad (2)$$

here, D is the updated duty ratio, D_1 is past duty ratio value, ΔD is the fraction update to the past value, $P(k)$ and $(k - 1)$ are the present and past powers of PV source, $V(k)$ and $V(k - 1)$ are the present and past voltages of PV source [9].

The wind farm boost converter is also controlled by MPPT algorithm with feedback from PMSG rotor angular speed w_r . The MPPT adopted for the wind farm unit is power signal feedback (PSF) control which generates optimal power estimation P_{opt} using PMSG rotor speed [12]. The similarity for the same is given:

$$P_{opt} = K_{opt} w_r^3 \quad (3)$$

here, K_{opt} is MPPT multiplication factor and w_r is the rotor speed of PMSG.

From the above optimal power reference generation required torque (T^*) is generated which is compared to measured electro-magnetic torque (T_e) of the machine. The error generated is fed to PI torque controller which generates duty ratio for the wind farm unit boost converter. The variable DC voltage generated by converting 3-ph PMSG voltages using diode bridge rectifier is now stabilized using boost converter operated by PSF MPPT algorithm [13], [14].

In the fuel cell unit, boost converter switch [15] is controlled using voltage constant (VC) feedback control which operates using reference voltage V_{ref} . This V_{ref} value is given as per the required voltage at the DC link which is determined as per the maximum voltage of the 3-ph grid. The same VC feedback control is also integrated to DC-DC bidirectional converter in battery unit which controls the buck and boost switch as per the available power. As per the control schematic Figure 3 V_{dc}^* is the reference voltage, V_{dc} measured voltage at the DC link, V_e is the error in voltage, Voltage controller is conventional PI controller [12], V_{cc} is the duty ratio, and m_d is the saw-tooth waveform.

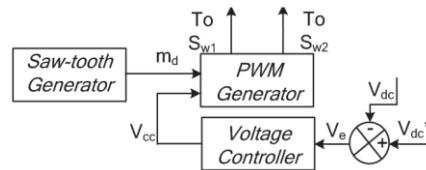


Figure 3. VC feedback control

The bidirectional converter [16] operates in buck mode when excess power is available storing energy in the battery pack. The same converter operates in boost mode when the system has insufficient compensation power. All the converters are synchronized to operate at same voltage at the DC link for optimal power extraction and sharing. The powers from the PV and wind farm units are completely extracted as they are natural resource generated powers. These powers are either injected to grid or stored in the battery as per the conditions in the system.

The battery unit is connected to the system when the grid is isolated considering it as a backup power source which supports the load. This triggering of battery unit is achieved using islanding detection algorithm which trips the circuit breaker of the battery as per the grid connection. During normal operating conditions when grid is connected, the load has support from the grid source therefore the battery unit is maintained disconnected. The fuel cell unit is operational when the battery unit is failed, or the battery unit cannot support the load. This fuel cell unit is triggered with feedback from battery state of charge (SOC) and load power. The fuel cell is triggered ON only in grid islanding and battery failure condition. The control modules for the inverter and the islanding detection algorithm are discussed in the next section.

3. 3-PH INVERTER CONTROL MODULES

The 3-ph inverter connected at the DC link is operated with different control techniques as per the grid connection. The 3-ph inverter is operated with SRF control when the renewable micro-grid is connected to main grid. The SRF controller takes feedback from DC link voltage, 3-ph grid voltages and inverter currents to make the inverter operate in synchronization to the grid. When the grid is disconnected (islanding condition) the 3-ph inverter needs to be operated with droop controller with voltage and frequency stability response. The droop control takes feedback from inverter voltage and angular frequency for injection of renewable power compensating the load. For the selection of inverter control technique as per the availability of grid, an islanding detection algorithm is used for switching between SRF and droop control modules. The internal modeling and structure of the control modules are discussed.

3.1. Islanding detection algorithm

This control module for detection of main grid connection to the renewable micro-grid takes feedback from grid voltage (V), frequency (f) and reactive power exchange (Q). The flowchart of the islanding detection algorithm [17] for switching between the control techniques is given in Figure 4. Initially measurements at PCC voltage (V_{pcc}) and load reactive power (Q_{load}) are taken with first comparison of the voltage magnitude within limits. The voltage magnitude comparison is given as if $0.88 V_n \leq V_{pcc} \leq 1.1 V_n$ - detect as grid connected or else grid islanding condition [18]. If the voltage is in given limits and if $V_{pcc} > V_n$, then Q_{ref} is calculated which is given as,

$$Q_{ref} = -\left(k_1 + \frac{V_{pcc} - V_n}{V_n} k_2\right) (f - x) + Q_{load} \tag{4}$$

after V_{pcc} magnitude comparison the frequency (f_{pcc}) of the V_{pcc} is checked to be in given limits and the comparison is given as $49.3 \leq f_{pcc} \leq 50.5$. If the frequency is not in the given limits the grid is in islanding state and the 3-phase inverter shifts from SRF to droop control module.

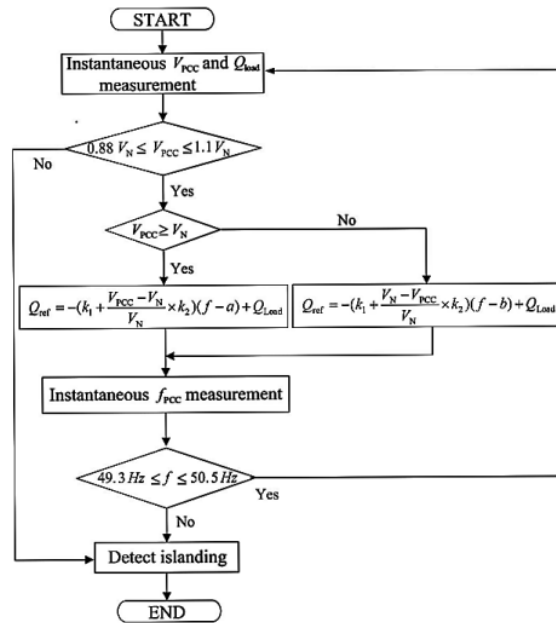


Figure 4. Islanding detection algorithm for controller switching

3.2. SRF control

The SRF control module [19] is conventional controller which takes feedback from PCC voltages, inverter currents and DC link voltage. This control module ensures that the renewable micro-grid injects power to the load or grid in synchronization to grid voltages. The conventional SRF control module can be seen in Figure 5.

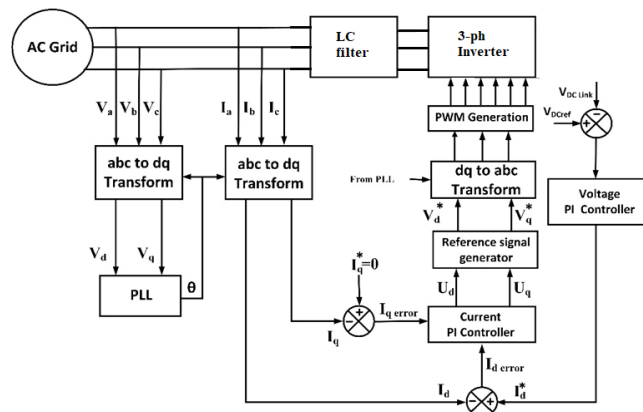


Figure 5. SRF control module during grid connected condition

As per the SRF control module [20] the reference d-q currents (I_d^* and I_q^*) are taken as ($I_d^*=0$) and I_q^* is calculated by voltage PI controller fed with DC link voltage comparison given as,

$$I_d^* = (V_{DC\ ref} - V_{dc\ link})(K_p + \int K_i \cdot dt) \tag{5}$$

here, K_p and K_i are the proportional and integral gains of the voltage controller. The reference d-q currents are compared to measured currents (I_d and I_q) which are generated by park's transformation given as,

$$\begin{bmatrix} I_d \\ I_q \end{bmatrix} = \frac{2}{3} \begin{bmatrix} \sin wt & \sin\left(wt - \frac{2\pi}{3}\right) & \sin\left(wt + \frac{2\pi}{3}\right) \\ \cos wt & \cos\left(wt - \frac{2\pi}{3}\right) & \cos\left(wt + \frac{2\pi}{3}\right) \end{bmatrix} \begin{bmatrix} I_a \\ I_b \\ I_c \end{bmatrix} \tag{6}$$

from the d-q error currents the reference signals U_d and U_q are generated which are used to get d-q reference signals (V_d^* and V_q^*) given as,

$$V_d^* = U_d + V_d + L\omega I_q \tag{7}$$

$$V_q^* = U_q + V_q - L\omega I_d \tag{8}$$

the above reference d-q components are converted back to abc sinusoidal reference signals using inverse park's transformation as given.

$$\begin{bmatrix} V_a \\ V_b \\ V_c \end{bmatrix} = \begin{bmatrix} \sin wt & \cos wt \\ \sin\left(wt - \frac{2\pi}{3}\right) & \cos\left(wt - \frac{2\pi}{3}\right) \\ \sin\left(wt + \frac{2\pi}{3}\right) & \cos\left(wt + \frac{2\pi}{3}\right) \end{bmatrix} \begin{bmatrix} V_d \\ V_q \end{bmatrix} \tag{9}$$

These reference sinusoidal waveforms are compared to high frequency triangular waveforms generating pulses for the 3-ph inverter. This technique is represented as sinusoidal pulse width-modulated (PWM) technique [15]. The angle (wt) in (6) and (9) are generated using PLL which is given input from grid voltages, this makes the 3-ph inverter to operate in synchronization to the grid.

3.3. Droop control

The droop control module controls the 3-ph inverter when the main grid is disconnected making the renewable micro-grid to operate in standalone condition [21]. As the renewable micro-grid is uncertain with powers and voltages because of unpredictable environmental conditions, it needs a voltage and frequency stabilizing controller. The droop control module considers an estimated required voltage signal with specific voltage magnitude and frequency. This reference signal is considered for PLL which is responsible for the calculation of d-q voltage and current components [21]. The complete internal structure of droop controller with conventional PI controller can be seen in Figure 6.

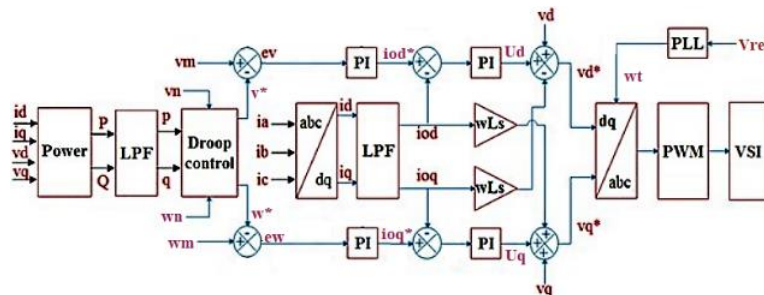


Figure 6. Proposed droop control structure

As per the given Figure 6 the $V_d V_q$ and $I_d I_q$ components are generated using (6) with 3-ph measurements taken after the LC filter of the 3-ph inverter. The 'wt' for the d-q component calculation is taken from reference voltage signal fed PLL unit [21]. From these d-q components the instantaneous real and reactive powers P and Q are calculated given as,

$$P = \frac{3}{2}(V_d I_d + V_q I_q) \quad (10)$$

$$Q = \frac{3}{2}(V_q I_d - V_d I_q) \quad (11)$$

with these real and reactive power components the reference angular frequency (w^*) and reference voltage magnitude (v^*) are calculated as,

$$w^* = w_n - k_w P \quad (12)$$

$$v^* = v_n - k_v Q \quad (13)$$

here, w_n is the fundamental angular frequency taken as $2\pi f$ where 'f' is 50 Hz and v_n is the fundamental voltage magnitude, k_w and k_v are the static droop coefficients which are depicted with,

$$k_w = \frac{w_{max} - w_{min}}{P_{max}} \quad (14)$$

$$k_v = \frac{v_{max} - v_{min}}{Q_{max}} \quad (15)$$

here, w_{max} and w_{min} are the maximum and minimum allowable angular frequency, v_{max} and v_{min} are the maximum and minimum allowable voltage magnitude [22] of the system, P_{max} is the maximum allowed real power and Q_{max} is the maximum allowed reactive power.

The reference current components ($i_{od}^* i_{oq}^*$) for generation of reference signals is given as,

$$i_{od}^* = (v^* - v_m)(K_p + \int K_i \cdot dt) \quad (16)$$

$$i_{oq}^* = (w^* - w_m)(K_p + \int K_i \cdot dt) \quad (17)$$

here, v_m and w_m are the measured voltage magnitude and angular frequency at the 3-ph inverter. The K_p and K_i are the proportional and integral gain values tuned as per the response of the system. With the reference current components, the voltage components ($U_d U_q$) are given as,

$$U_d = (i_{od}^* - i_{od})(K_p + \int K_i \cdot dt) \quad (18)$$

$$U_q = (i_{oq}^* - i_{oq})(K_p + \int K_i \cdot dt) \quad (19)$$

from these voltage components ($U_d U_q$) the final reference voltage signals ($v_d^* v_q^*$) for PWM pulse generation are given as,

$$v_d^* = v_d + U_d - i_{oq} w L_s \quad (20)$$

$$v_q^* = v_q + U_q + i_{od} w L_s \quad (21)$$

here, L_s is the inverter filter inductance and w is the considered angular frequency taken as $2\pi f$.

The $v_d^* v_q^*$ are transformed to V_{abc} reference signals by using (9) and these signals are compared to high frequency triangular waveform generating PWM pulses [23] controlling the 3-ph voltage source inverter (VSI). For further stabilization the traditional PI controller is updated with FIS control module for better stability of the inverter during grid islanding and load variation condition.

3.4. FIS control module

The FIS module is a stabilization controller for better control over the current components generated by the comparison of voltage magnitude and angular frequency signals. The traditional PI controller is replaced by the FIS control module which is designed with two input signals error (e), change in error (ce) and one output signal (o) [24]. Each considered signal has seven membership functions which are defined in specific limits as per the input value. The structures of the seven membership functions in each variable can be seen in Figure 7.

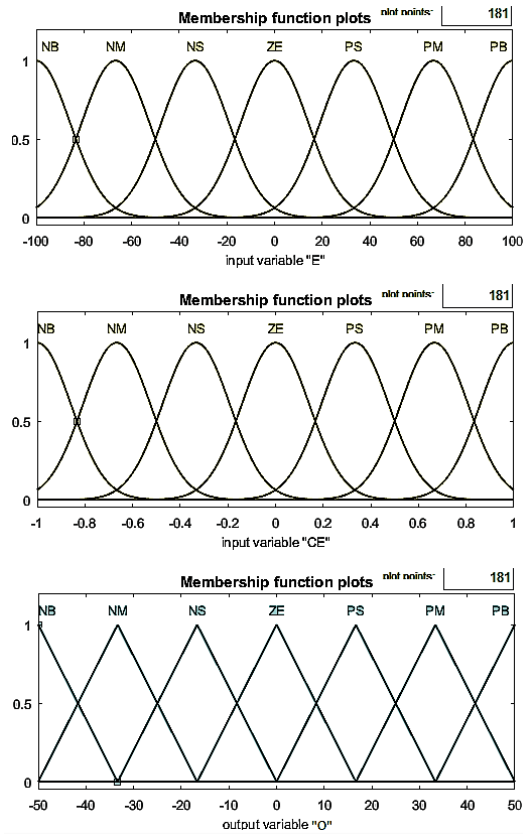


Figure 7. FIS variables membership functions

The limits of the variables are set as per the response of the controller to the changes in the system. The output currents ($i_{od}^* i_{oq}^*$) are generated with respect to given 7x7 rule base [25] in Table 1. The output currents ($i_{od}^* i_{oq}^*$) are further processed as per conventional controller in Figure 6 for the generation of reference signals V_{abc} . As the reference currents are stabilized with FIS control, the 3-ph inverter signals are also stabilized with faster response rate. This makes the 3-ph inverter to maintain the system with stable voltage and frequency as per the V_{ref} signal given. A comparative analysis of the test system with renewable micro-grid operated with different droop control modules is done. Multiple parameters are compared with simulation design using PI, PID, and FIS controllers in further section.

Table 1. 7x7 rule base

ce	e						
	NB	NM	NS	ZE	PS	PM	PB
PB	Z	PS	PM	PB	PB	PB	PB
PM	NS	Z	PS	PM	PB	PB	PB
PS	NB	NS	Z	PS	PM	PB	PB
ZE	NB	NM	NS	Z	PS	PM	PB
NS	NB	NB	NM	NS	Z	PS	PM
NM	NB	NB	NB	NM	NS	Z	PS
NB	NB	NB	NB	NB	NM	NS	Z

4. SIMULATION ANALYSIS

The complete system with main grid connected to four renewable source micro-grid is modeled using MATLAB Simulink environment. An isolation circuit breaker for main grid disconnection to create islanding condition is used. Islanding detection algorithm is integrated to PCC voltage and reactive power for detection of grid disconnection tripping the controller of the 3-ph inverter from SRF to droop controller. The complete system is modeled with the system parameters taken from Table 2 which include ratings of the renewable sources and change in operating conditions.

Table 2. System parameters

Name of the parameter	Values
Grid rating	11 kV, 50 Hz, 100 MVA
Load parameters	L1 – 30 kW, L2 – 20 kW
PV module	$V_{mp} = 54.7V$, $I_{mp} = 5.58 A$, $V_{oc} = 64.2 V$, $I_{sc} = 5.96 A$, $N_p = 10$, $N_s = 5$. $P_{pv\ total} = 15 kW$, Boost converter – $L_b = 1 mH$, $C_{in} = 100 \mu F$, $C_{out} = 12 mF$.
Wind farm module	PMSG – 67 N-mt, 560 Vdc, 1700 rpm Turbine – 12 kW, Base wind speed = 12 m/s, base rotational speed = 1.2 pu Boost converter – $L_b = 100 \mu H$, $C_{in} = 1000 \mu F$, $C_{out} = 1000 \mu F$
BESS module	Lithium-Ion $V_{nom} = 250 V$, Capacity = 100 Ah Bidirectional converter - $L_b = 161.95 \mu H$, $C_{out} = 220 \mu F$
Fuel cell module	$V_{nom} = 300 V$, $I_{nom} = 133.3 A$, $V_{end} = 220V$, $I_{end} = 225 A$. Boost converter – $L_b = 1 mH$, $C_{in} = 100 \mu F$, $C_{out} = 12 mF$.
VSI LC filter	$L_f = 250 mH$, $C_f = 2.6 kVAR$
Islanding detection limits	$0.88 < V_{mag} < 1.1$, $-1 > Q > 1$, $49.3 < f < 50.5$
SRF controller gains	DC voltage gains - $K_p = 7$, $K_i = 800$ Current controller gains – $K_p = 0.3$, $K_i = 20$
Drop controller gains	V & w controller gains – $K_p = 0.05$, $K_i = 0.01$ Current controller gains – $K_p = 0.3$, $K_i = 20$

The system parameters are considered as per the load demand and the general voltage values considered in a grid system. With the given parameters in Table 2 the modeling of the test system is done in MATLAB Simulink environment and the complete modeling diagram can be seen in Figure 8. The simulation is run for 5 sec with different operating conditions in specific intervals of time. The main grid is disconnected at 0.5 sec using a circuit breaker, making the renewable micro-grid to operate in islanding condition from 0.5 sec. Therefore at 0.5 sec the 3-ph VSI controller shifts from SRF controller to droop controller. Now as the main grid is disconnected, battery energy storage system (BESS) module is activated supporting the system. At 1.2 sec the solar irradiation is varied from 1000 W/m² to 500 W/m² reducing the solar power generation.

At 2 sec load L2 of 20 kW is connected along with previous load L1 30 kW added up to 50 kW total load. This excess load demand is supported by BESS module from 2 sec. In the next instance at 3.5 sec the BESS module is disconnected creating BESS failure, making the fuel cell module to connect at 3.5 sec. All the power and voltage graphs with different controllers (PI, PID, and FIS) are shown for the given operating conditions. The Figure 9 is the 3-ph PCC voltages and micro-grid currents which have a change at 0.5 sec, the voltage swells until 0.7 sec and then it is stabilized by the droop controller. For the conditions in the test system mentioned previously, the active powers of the all the modules are shown in Figure 10. The values of the active powers of each module are mentioned with respect to time range in Table 3.

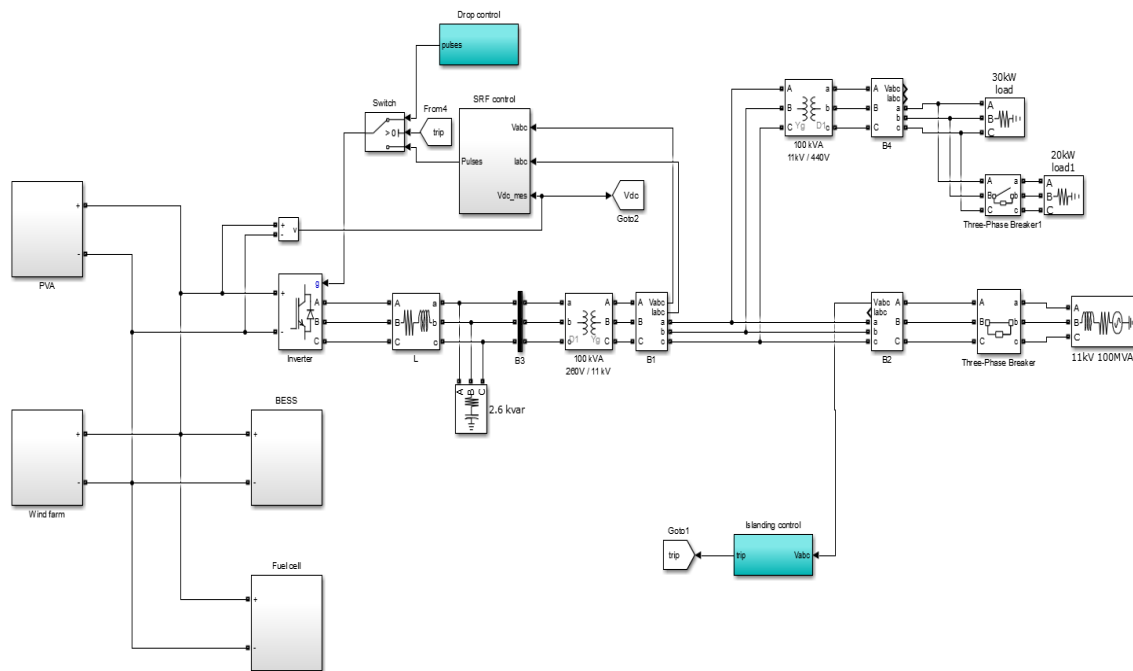


Figure 8. Simulink modeling of the proposed test system

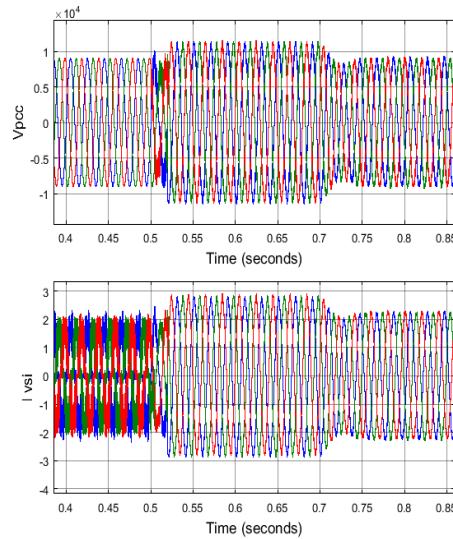


Figure 9. 3-ph PCC voltages and renewable micro-grid currents

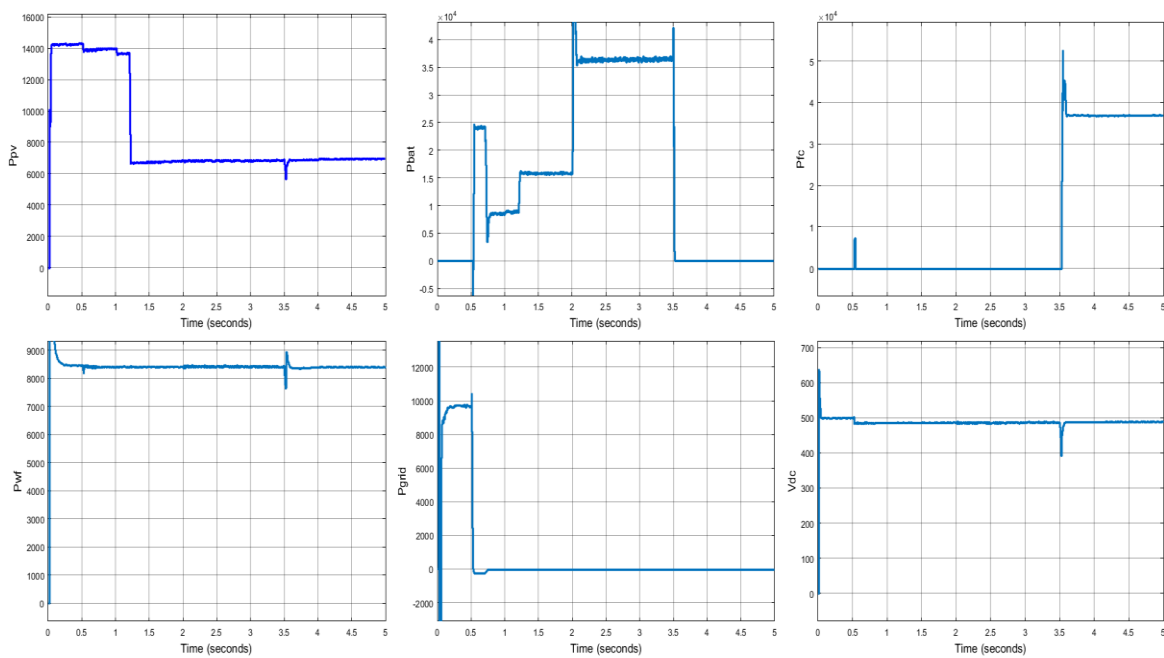


Figure 10. Active power of all modules and DC link voltage

Table 3. Active powers of all modules

Parameter	0-.5 sec	0.5-.2 sec	1.2-2 sec	2-3.5 sec	3.5-5 sec
Ppv	14 kW	14 kW	7 kW	7 kW	7 kW
Pwf	8.5 kW	8.5 kW	8.5 kW	8.5 kW	8.5 kW
Pgrid	10 kW	0	0	0	0
Pbat	0	10 kW	15 kW	36 kW	0
Pfc	0	0	0	0	36 kW
Pload	30 kW	30 kW	30 kW	50 kW	50 kW

The load and MG active power compensation with different droop controllers (PI, PID, and FIS) can be seen in Figure 11. The response of the FIS controller droop control module has faster response as compared to PI, PID, and maintains the power at 50 kW from 3.5 sec when the battery is failed. The other two controllers have slower response and can compensate only 46 kW for 50 kW load demand after 3.5 sec.

The Figure 12 is the DC link voltage and PCC voltage magnitude comparison measured on the DC side of the 3-ph VSI which is mostly stable and has less ripple for FIS droop control. The magnitude of the voltage also tends to maintain near to 500 V (490 V) in any given condition. The other two controllers (PI PID) have higher ripple in the voltage from 2-3.5 sec and the magnitude is dropped to 470 V when the battery is failed.

Even the voltage magnitude on the AC side at PCC the FIS droop control modules maintain the voltage always around 1 pu for any given condition. On the other hand, the voltage magnitude at PCC is varying from 1.02 pu to 0.97 pu when operated with PI or PID. Along with the voltage magnitude the frequency of the PCC voltage is also stabilized with less ripple and faster settling time for FIS droop control which can be seen in Figure 13 as seen the frequency after 1 sec for FIS droop control is settling faster and tends to maintain at 50 Hz and with lower ripple content as compared to PI or PID. The Table 4 is the comparison of parameters when the system is operated with different controllers.

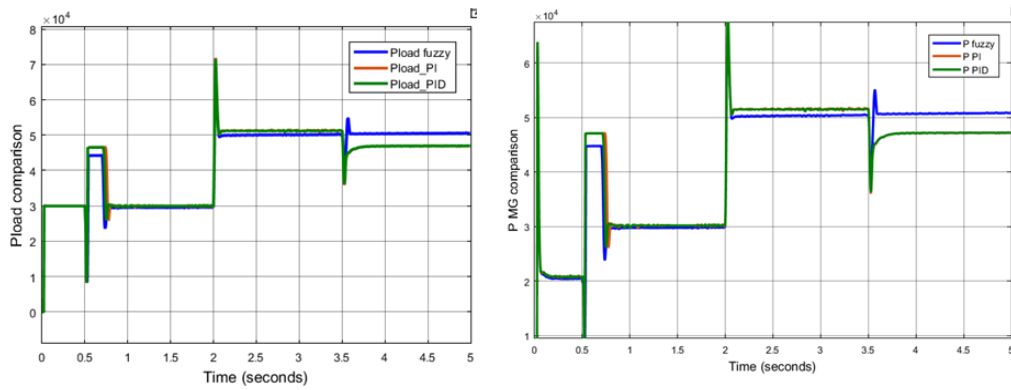


Figure 11. Load and MG active power comparison

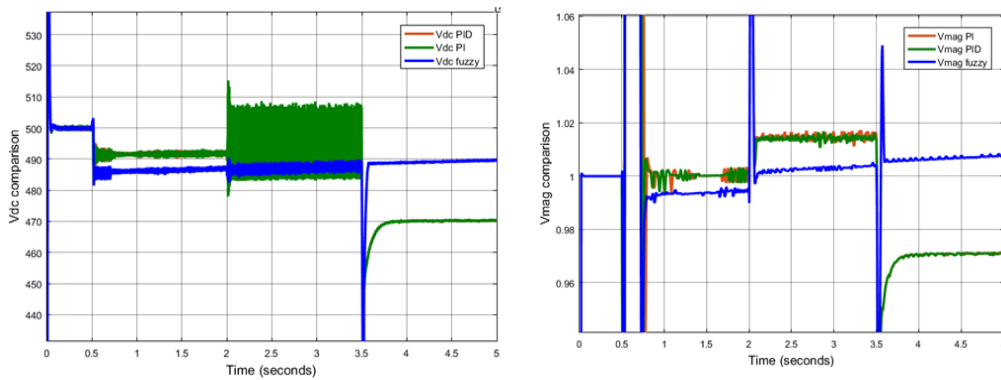


Figure 12. DC link voltage and V_{pcc} voltage magnitude comparison

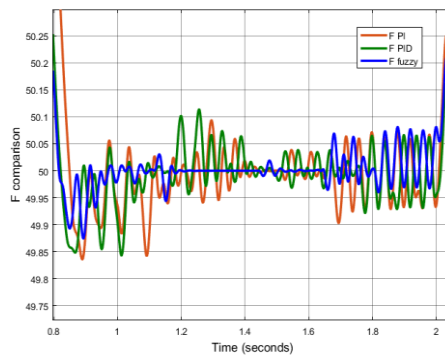


Figure 13. V_{pcc} voltage frequency comparison

Table 4. Parametric comparison

Name of the parameter	PI	PID	FIS
P-MG	46 kW	46 kW	50k W
Vdc ripple %	4.92%	4.92%	0.81%
Vdc magnitude	470 V	470 V	490 V
Vpcc magnitude	1.05 pu	0.97 pu	0.97 pu
F settling time	0.9 sec	0.9 sec	0.5 sec
F ripple %	0.5%	0.2%	0.2%

5. CONCLUSION

As per the given results the system parameters like power, voltage magnitude and frequency are more stable when the inverter is operated with FIS controlled droop controller. This proposed droop controller has faster response time with reduced disturbances in the system parameters when operated in standalone condition. The power balancing is also achieved compensating the load power by the backup modules BESS or fuel cell. As per the calculated values of different parameters in the system it can be concluded that the complete system is more stable when the inverter is operated with FIS integrated droop control. There is a very high mitigation in ripple of the voltages, full compensation of required load power and reduction of settling time of the parameters. The number of renewable sources can be increased in further development reducing stress on the battery backup device. Better stable controller modules can be integrated for more stability and faster response to the changes in the grid system.

REFERENCES

- [1] M. H. Saeed, W. Fangzong, B. A. Kalwar, and S. Iqbal, "A review on microgrids' challenges perspectives," *IEEE Access*, vol. 9, pp. 166502–166517, 2021, doi: 10.1109/ACCESS.2021.3135083.
- [2] C. Zhang, Y. Xu, and Z. Y. Dong, "Robustly coordinated operation of a multi-energy micro-grid in grid-connected and islanded modes under uncertainties," *IEEE Transactions on Sustainable Energy*, vol. 11, no. 2, pp. 640–651, Apr. 2020, doi: 10.1109/TSTE.2019.2900082.
- [3] A. Zhou, R. Yan, and T. K. Saha, "Capacity and control strategy design of isolated micro-grid with high renewable penetration," *IEEE Transactions on Sustainable Energy*, vol. 11, no. 3, pp. 1173–1184, Jul. 2020, doi: 10.1109/TSTE.2019.2920274.
- [4] F. Dubuisson, M. Rezkallah, A. Chandra, and M. Tremblay, "Control of a new standalone microgrid configuration," in *Canadian Conference on Electrical and Computer Engineering*, May 2018, vol. 2018-May, pp. 1–4, doi: 10.1109/CCECE.2018.8447704.
- [5] G. T. Hasan, A. H. Mutlaq, and M. O. Salih, "Investigate the optimal power system by using hybrid optimization of multiple energy resources software," *Indonesian Journal of Electrical Engineering and Computer Science (IJECS)*, vol. 26, no. 1, pp. 9–19, Apr. 2022, doi: 10.11591/ijeecs.v26.i1.pp9-19.
- [6] G. Escobar, L. Ibarra, J. E. V. Resendiz, J. C. M. Maldonado, and D. Guillen, "Nonlinear stability analysis of the conventional SRF-PLL and enhanced SRF-EPLL," *IEEE Access*, vol. 9, pp. 59446–59455, 2021, doi: 10.1109/ACCESS.2021.3073063.
- [7] R. K. Sharma, S. Mudaliyar, and S. Mishra, "A DC droop-based optimal dispatch control and power management of hybrid photovoltaic-battery and diesel generator standalone AC/DC system," *IEEE Systems Journal*, vol. 15, no. 2, pp. 3012–3023, Jun. 2021, doi: 10.1109/JSYST.2020.3032887.
- [8] M. S. B. Z. Abidin, N. B. Salim, A. N. B. Azmi, N. A. B. Zambri, and T. Tsuji, "Frequency control reserve with multiple micro grid participation for power system frequency stability," *Indonesian Journal of Electrical Engineering and Computer Science (IJECS)*, vol. 16, no. 1, pp. 59–66, Oct. 2019, doi: 10.11591/ijeecs.v16.i1.pp59-66.
- [9] B. Jyothi, P. Bhavana, B. T. Rao, and M. S. K. Reddy, "A review on various DC-DC converters for photo voltaic based DC micro grids," in *2021 IEEE International Conference on Emerging Trends in Industry 4.0, ETI 4.0 2021*, May 2021, pp. 1–8, doi: 10.1109/ETI4.051663.2021.9619280.
- [10] Z. Chen, K. Wang, Z. Li, and T. Zheng, "A review on control strategies of AC/DC micro grid," in *Conference Proceedings - 2017 17th IEEE International Conference on Environment and Electrical Engineering and 2017 1st IEEE Industrial and Commercial Power Systems Europe, EEEIC / I and CPS Europe 2017*, Jun. 2017, pp. 1–6, doi: 10.1109/EEEIC.2017.7977807.
- [11] A. Nigam and A. K. Gupta, "Performance and simulation between conventional and improved perturb & observe MPPT algorithm for solar PVcell using MATLAB/Simulink," in *ICCCCM 2016 - 2nd IEEE International Conference on Control Computing Communication and Materials*, Oct. 2017, pp. 1–4, doi: 10.1109/ICCCCM.2016.7918220.
- [12] H. M. A. Alhussain and N. Yasin, "Modeling and simulation of solar PV module for comparison of two MPPT algorithms (P&O & INC) in MATLAB/Simulink," *Indonesian Journal of Electrical Engineering and Computer Science (IJECS)*, vol. 18, no. 2, pp. 666–677, May 2020, doi: 10.11591/ijeecs.v18.i2.pp666-677.
- [13] H. S. Shin, C. Xu, J. M. Lee, J. Du La, and Y. S. Kim, "MPPT control technique for a PMSG wind generation system by the estimation of the wind speed," in *ICEMS 2012 - Proceedings: 15th International Conference on Electrical Machines and Systems*, 2012, pp. 1–6.
- [14] A. Belkacem, Z. Boudjema, G. Bachir, and R. Taleb, "Advanced control of a permanent magnet synchronous generator for a wind turbine," *Indonesian Journal of Electrical Engineering and Computer Science*, vol. 26, no. 1, pp. 194–201, Apr. 2022, doi: 10.11591/ijeecs.v26.i1.pp194-201.
- [15] M. Hassan, C. L. Su, F. Z. Chen, and K. Y. Lo, "Adaptive passivity-based control of a DC-DC boost power converter supplying constant power and constant voltage loads," *IEEE Transactions on Industrial Electronics*, vol. 69, no. 6, pp. 6204–6214, Jun. 2022, doi: 10.1109/TIE.2021.3086723.
- [16] R. D. Bhagiya and D. R. M. Patel, "PWM based double loop PI control of a bidirectional DC-DC converter in a standalone PV/Battery DC power system," in *2019 IEEE 16th India Council International Conference, INDICON 2019 - Symposium Proceedings*, Dec. 2019, pp. 1–4, doi: 10.1109/INDICON47234.2019.9028974.
- [17] X. Chen and Y. Li, "An islanding detection algorithm for inverter-based distributed generation based on reactive power control," *IEEE Transactions on Power Electronics*, vol. 29, no. 9, pp. 4672–4683, Sep. 2014, doi: 10.1109/TPEL.2013.2284236.

- [18] E. J. Estebanez, V. M. Moreno, A. Pigazo, M. Liserre, and A. Dell'Aquila, "Performance evaluation of active islanding-detection algorithms in distributed-generation photovoltaic systems: two inverters case," *IEEE Transactions on Industrial Electronics*, vol. 58, no. 4, pp. 1185–1193, Apr. 2011, doi: 10.1109/TIE.2010.2044132.
- [19] Z. Alqarni and J. A. Asumadu, "Synchronized power injection from PVA to grid with reduced THD and DC voltage ripple using PID controller for DC grid applications," in *2020 10th Annual Computing and Communication Workshop and Conference, CCWC 2020*, Jan. 2020, pp. 248–256, doi: 10.1109/CCWC47524.2020.9031111.
- [20] T. A. Jumani, M. W. Mustafa, M. M. Rasid, N. H. Mirjat, Z. H. Leghari, and M. S. Saeed, "Optimal voltage and frequency control of an islanded microgrid using grasshopper optimization algorithm," *Energies*, vol. 11, no. 11, Nov. 2018, doi: 10.3390/en11113191.
- [21] J. R. Reddy, A. Pandian, R. Dhanasekharan, C. R. Reddy, B. P. Lakshmi, and B. N. Devi, "Islanding detection of integrated distributed generation with advanced controller," *Indonesian Journal of Electrical Engineering and Computer Science (IJECS)*, vol. 17, no. 3, pp. 1626–1631, Mar. 2020, doi: 10.11591/ijeecs.v17.i3.pp1626-1631.
- [22] R. Mahmud, M. A. Hossain, and H. Pota, "Nonlinear output feedback droop control for parallel inverters in standalone microgrids," in *2019 9th International Conference on Power and Energy Systems, ICPEs 2019*, Dec. 2019, pp. 1–6, doi: 10.1109/ICPEs47639.2019.9105385.
- [23] R. K. Sharma and S. Mishra, "Dynamic power management and control of a PV PEM fuel-cell-based standalone ac/dc microgrid using hybrid energy storage," *IEEE Transactions on Industry Applications*, vol. 54, no. 1, pp. 526–538, Jan. 2018, doi: 10.1109/TIA.2017.2756032.
- [24] L. C. Duttu, G. Mauris, and P. Bolon, "A fast and accurate rule-base generation method for mamdani fuzzy systems," *IEEE Transactions on Fuzzy Systems*, vol. 26, no. 2, pp. 715–733, Apr. 2018, doi: 10.1109/TFUZZ.2017.2688349.
- [25] Y. Krim, D. Abbes, S. Krim, and M. F. Mimouni, "Fuzzy droop control for voltage source inverter operating in standalone and grid connected modes," in *2018 15th International Multi-Conference on Systems, Signals and Devices, SSD 2018*, Mar. 2018, pp. 1110–1116, doi: 10.1109/SSD.2018.8570669.

BIOGRAPHIES OF AUTHORS



Savitri Swathi    is research scholar at Electrical Engineering Department University College of Engineering, Osmania University. She is working as Assistant Professor in Institute of Aeronautical Engineering College From 2012 Dundigal, Hyderabad. She guided 2 PG and 4 UG projects. Her research areas are power system, power quality, and power electronics. She can be contacted at email: eee.swathi48@gmail.com.



Dr. Bhaskaruni Suresh Kumar    is Associate Professor at Electrical and Electronics Engineering Department in Chaitanya Bharathi Institute of Technology, Osmania University. He holds a PhD degree in Power Quality-Power Systems in the year 2014 from JNTU Kukatpally, Hyderabad, Telangana. His research areas are power system, and power quality. He can be contacted at email: bskbus@gmail.com.



Dr. Jalla Upendar    is Assistant Professor at Electrical Engineering Department University College of Engineering, Osmania University. He holds a PhD degree in Intelligent Approach for Fault Classification of Power Transmission Systems with specialization in Electrical Engineering in Indian Institute of Technology (IIT), Roorkee, Uttarakhand, India in 2010. His research areas are power system, power electronics, FACTS devices, and artificial intelligent techniques. He can be contacted at email: dr.8500003210@gmail.com.